YIELDING OF ROTATING TWO-LAYER COMPOSITE TUBES

A THESIS SUBMITTED TO

THE GRADUATE SCHOOL OF NATURAL AND APPLIED SCIENCES

OF

ATILIM UNIVERSITY

BY

MEHMET DALKILIÇ

IN PARTIAL FULFILLMENT OF THE REQUIREMENTS FOR THE DEGREE OF

MASTER OF SCIENCE

IN

THE DEPARTMENT OF CIVIL ENGINEERING

APRIL 2009

Approval of the Graduate School of Natural and Applied Sciences, Atılım University.

_____

Prof.Dr. Abdurrahim Özgenoğlu
Director

I certify that this thesis satisfies all the requirements as a thesis for the degree of Master of Science.

_____

Prof.Dr. Selçuk Soyupak
Head of Department

This is to certify that we have read the thesis "Yielding Of Rotating Two-Layer Composite Tubes" submitted by Mehmet Dalkılıç and that in our opinion it is fully adequate, in scope and quality, as a thesis for the degree of Master of Science.

_____

Asst.Prof.Dr. Tolga Akış
Supervisor

Examining Committee Members

Asst. Prof. Dr. Hakan Argeşo
Manuf. Eng. Dept., Atılım University _____

Asst. Prof. Dr. Tolga Akış
Civil Eng. Dept., Atılım University _____

Asst. Prof. Dr. Eray Baran
Civil Eng. Dept., Atılım University _____

Date: April 27, 2009

I declare and guarantee that all data, knowledge and information in this document has been obtained, processed and presented in accordance with academic rules and ethical conduct. Based on these rules and conduct, I have fully cited and referenced all material and results that are not original to this work.

Name, Last name: Mehmet Dalkılıç

Signature:

ABSTRACT

YIELDING OF ROTATING TWO-LAYER COMPOSITE TUBES

Dalkılıç, Mehmet

M.S., Civil Engineering Department

Supervisor: Asst. Prof. Dr. Tolga Akış

April 2009, 37 pages

The purpose of this study is to present an analytical approach for the elastic analysis of rotating two-layer composite tubes. The expressions of stresses and displacement are obtained and the critical cases of yielding are examined using von Mises yield criterion. The analytical solutions are also checked numerically for material sets and stress and displacement distributions are obtained under rotation. It is found that yielding may begin at the inner surface of the assembly, or at the interface of the two tubes, or as a special case, simultaneously at the inner surfaces of both tubes.

Key words: Stress analysis; Rotating tube; von Mises criterion

ÖZ

DÖNEN İKİ KATMANLI KOMPOZİT TÜPLERİN AKMASI

Dalkılıç, Mehmet

Yüksek Lisans, İnşaat Mühendisliği Bölümü

Tez Danışmanı: Yrd. Doç. Dr. Tolga Akış

Nisan 2009, 37 sayfa

Bu çalışmanın amacı, dönen iki katmanlı kompozit tüplerin elastik analizi için analitik bir yaklaşım sunmaktır. Gerilme ve yer değiştirmelere ait ifadeler elde edilmiş ve kritik akma koşulları von Mises akma kriteri kullanılarak incelenmiştir. Analitik çözümler ayrıca çeşitli malzeme setleri için uygulanmış ve dönme etkisi altındaki gerilme ve yer değiştirme dağılımları bulunmuştur. Akmanın sistemin iç yüzeyinden, iki tüpün etkileşim yüzeyinden veya özel bir durum olarak, iki tüpün iç yüzeylerinden eş zamanlı başlayabileceği bulunmuştur.

Anahtar Kelimeler: Gerilme analizi; Dönen tüp; von Mises kriteri

To My Family

ACKNOWLEDGEMENTS

I express sincere appreciation and thanks to my supervisor Asst. Prof. Dr. Tolga Akış for his guidance, insight, and endless patience throughout the research. To my wife, İpek, I offer sincere thanks for her continuous encouragement and patience during this period. And to my parents and brother, who gave their constant love and support for my whole life, I am grateful for helping me becoming who I am.

TABLE OF CONTENTS

LIST OF TABLES

TABLES

LIST OF FIGURES

FIGURES

LIST OF SYMBOLS

r , θ , z	cylindirical polar coordinates
a , r_1 , b	inner, interface and outer radii of the composite tube
$\overline{a}$, $\overline{r}_1$	dimensionless inner and interface radii of the composite tube
C_i	integration constants
E	modulus of elastcity
ν	Poisson's ratio
$\overline{r}$	dimensionless radial coordinate
u	radial displacement
$\overline{u}$	dimensionless radial displacement
ε_i	strain components
$\overline{\varepsilon}_i$	normalized strain components
ϕ_i	non-dimensional stress variable
σ_i	stress components
$\overline{\sigma}_i$	dimensionless stress components
σ_0 , σ_Y	initial and subsequent yield stress
ω	angular velocity
Ω	dimensionless angular velocity
Ω_e	dimensionless elastic limit angular velocity

CHAPTER I

INTRODUCTION

The analysis of rotating members (shafts, annular disks, tubes, etc.) gathers extensive interest due to applicational importance in engineering. Such elements are used in several mechanical designs from electrical motors to turbine rotors, from heat furnaces to fly-wheels. Among them, the stress analysis of rotating shafts attracts the attention of the researchers as a basic mechanical problem. The formulations of the stresses and displacements for such elements under different conditions are given in many text books [1-3]. Besides these, studies on the elastic and elastic-plastic analysis of rotating solid and hollow shafts (tubes) are performed by several researchers. In addition, two-layer composites tubes under different loading conditions are studied in the past.

Focusing only on the stress distribution in the rotating elastic-plastic hollow shafts, the analytical solution developed by Gamer and Lance [4] explains rigorously the fixed end tube behaviour, using Tresca's yield condition. In a later study, Mack [5] presented the elastic-plastic tube solution for free ends, again implementing Tresca's yield criterion. In this complicated study Mack developed analytical solutions demonstrating the development of plastic regions and examined the behaviour at the elastic-plastic borders as well.

The problem of rotating elastic-plastic solid shafts is studied by Mack [6] for free ends and by Gamer et al. [7] for fixed end conditions. Both papers examined the

elastic and elastic-plastic stresses, strains and displacement in a rotating solid cylinder based on Tresca's yield criterion and the flow rule associated with it. The development of the plastic regions and the transition from the elastic state to the perfectly plastic state are investigated as well as the full plastic behaviour, especially in the latter paper. In a study by Eraslan [8], the behaviour of nonlinearly hardening rotating shafts is examined using von Mises' yield criterion. In the study, a comparison of the result with the existing analytical solutions from other studies based on Tresca's criterion is made in order to verify the model and to compare the most common two yield criteria. The solutions and procedure are developed for both hollow and solid shafts and for free and fixed end conditions as well. Another study on the rotating elastic-plastic shafts is made by Eraslan and Mack [9] concerning the computational procedures to be implemented for all types of shafts (hollow-solid, free end-fixed end). This paper utilizes von Mises' yield criterion and presents an efficient investigation especially by taking into account the nonlinear strain hardening. Estimating the residual stresses and secondary plastic flows limits are also of particular interest.

On the other hand, in closely related studies, two layer tubes under different loading conditions are investigated. Akış and Eraslan [10] studied a plane strain tube problem in elastic stress state under internal and external radial pressure for tightly fitted two layer tubes with fixed ends, and Eraslan and Akış [11] analyzed the same problem in elastic-plastic stress state. Another study on composite tubes by Eraslan and Akış [12] covers the same subject for pressurized shrink-fitted tubes. In all these works, either external or internal pressure is applied and von Mises' criterion is used for monitoring the yielding.

Another interesting subject, the stresses developed in rotating solid shafts made of functionally graded materials are studied extensively in several works by Akış and Eraslan [13-15] in both elastic and elastic-plastic stress states. A radially varying modulus of elasticity and uniaxial yield limit is assumed for the shaft and closed form solutions are developed for the model, examining the possibilities of performance improvements for functionally graded material shafts. This subject also studied in a work by Argeşo and Eraslan [16] using a computational approach and verifying with analytical solutions available in the literature.

It is known from the literature that the yielding behaviour of the rotating two-layer composite tubes has not yet been investigated thoroughly. Therefore, the aim of this study is to obtain consistent analytical solutions to this problem and determine the conditions of the yielding of the assembly.

Two tightly-fitted tubes having different material properties are considered in this study. A long tube of inner radius a and outer radius r_1 is placed in a tube of the same length of inner radius r_1 and outer radius b. In the derivations r_1 is defined as the interface radius. The geometry of the assembly is shown in Figure 1.1. In the study, the subscripts 1 and 2 are used to denote the material properties (E, ν, σ_0) of the inner and outer tubes, respectively.

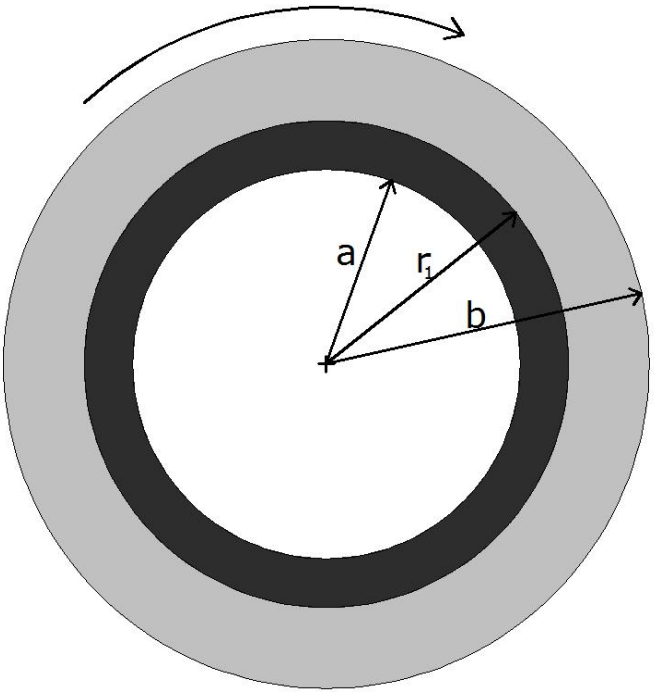

Figure 1.1 The section of the two-layer tube assembly

In Chapter II, the analytical expressions for the stresses and displacement are derived starting with a single tube problem which is covered widely in the literature. Using this single tube solution, the expressions for the two-layer tubes are obtained. In addition to these, von Mises criterion is determined for the tube assembly for monitoring the yielding behaviour.

As the yielding of a single layer tube starts from the inner surface, it is expected that the yielding may begin at the inner surface of the tube assembly. However, since there are two tubes, it is also possible that the yielding may commence first at the inner surface of the outer tube, which is the interface r_1. Or as a special case, yielding may begin at the inner surfaces of both tubes simultaneously. The numerical results for all these conditions are presented in Chapter III. Finally in the last chapter, a brief summary together with a conclusion part is given.

CHAPTER II

FORMULATION AND SOLUTION

2.1 General

Cylindrical polar coordinates (r, θ, z) are used in all derivations. It is assumed that the ends of the assembly are axially constrained. First, the governing equations for a rotating single tube are derived. Then, the relations regarding the inner and outer layers of the composite tube under rotation are given. Finally, the yielding behaviour due to von Mises yield criterion is presented.

2.2 Single Tube Under Rotation

The equilibrium equation for a rotating single tube in radial direction

$$\frac{d}{dr}(r\sigma_r) - \sigma_\theta + \rho\omega^2 r^2 = 0\,, \tag{1}$$

the generalized Hooke's Law

$$\varepsilon_r = \frac{1}{E}\left[\sigma_r - \nu(\sigma_\theta + \sigma_z)\right], \tag{2}$$

$$\varepsilon_\theta = \frac{1}{E}\left[\sigma_\theta - \nu(\sigma_r + \sigma_z)\right], \tag{3}$$

$$\varepsilon_z = \frac{1}{E}\left[\sigma_z - \nu(\sigma_r + \sigma_\theta)\right], \tag{4}$$

and the compatibility relation

$$\varepsilon_r = \frac{d}{dr}(r\varepsilon_\theta) \tag{5}$$

are the basic relations of the problem [1]. In addition, the following dimensionless and normalized variables are used:

$$\bar{r} = \frac{r}{b},\ d\bar{r} = \frac{dr}{b},\ \bar{\sigma}_i = \frac{\sigma_i}{\sigma_0},\ \Omega^2 = \frac{\omega^2 b^2 \rho}{\sigma_0},\ \bar{\varepsilon}_i = \frac{\varepsilon_i E}{\sigma_0}. \tag{6}$$

In view of these, the dimensionless form of the equilibrium equation becomes

$$\frac{d}{d\bar{r}}(\bar{r}\bar{\sigma}_r) - \bar{\sigma}_\theta + \Omega^2\bar{r}^2 = 0\,, \tag{7}$$

and the generalized Hooke's Law will be

$$\bar{\varepsilon}_r = \bar{\sigma}_r - \nu(\bar{\sigma}_\theta + \bar{\sigma}_z)\,, \tag{8}$$

$$\bar{\varepsilon}_\theta = \bar{\sigma}_\theta - \nu(\bar{\sigma}_r + \bar{\sigma}_z)\,, \tag{9}$$

$$\bar{\varepsilon}_z = \bar{\sigma}_z - \nu(\bar{\sigma}_r + \bar{\sigma}_\theta)\,. \tag{10}$$

For axially constrained ends $\bar{\varepsilon}_z = 0$ and the axial stress component becomes $\bar{\sigma}_z = \nu(\bar{\sigma}_r + \bar{\sigma}_\theta)$. Introducing the stress function $Y = \bar{r}\bar{\sigma}_r$, substituting the stress components $\bar{\sigma}_r$ and $\bar{\sigma}_\theta$ into the equation of equilibrium (7) and using the compatibility relation (5) one finds

$$\bar{r}^2 \frac{d^2Y}{d\bar{r}^2} + \bar{r}\frac{dY}{d\bar{r}} - Y = -\frac{\bar{r}^3\Omega^2(3-2\nu)}{1-\nu}. \tag{11}$$

The solution of this differential equation for Y is

$$Y = \frac{C_1}{\bar{r}} + C_2\bar{r} - \frac{\bar{r}^3\Omega^2(3-2\nu)}{8(1-\nu)}, \tag{12}$$

and the radial stress component becomes

$$\bar{\sigma}_r = \frac{C_1}{\bar{r}^2} + C_2 - \frac{\bar{r}^2\Omega^2(3-2\nu)}{8(1-\nu)}. \tag{13}$$

Here C_1 and C_2 are the integration constants. Using the equation of equilibrium, the circumferential stress component can be obtained as

$$\bar{\sigma}_\theta = -\frac{C_1}{\bar{r}^2} + C_2 - \frac{\bar{r}^2\Omega^2(1+2\nu)}{8(1-\nu)}. \tag{14}$$

Finally, using $\bar{\sigma}_z = \nu(\bar{\sigma}_r + \bar{\sigma}_\theta)$, the axial stress becomes,

$$\bar{\sigma}_z = 2C_2\nu - \frac{\bar{r}^2\Omega^2\nu}{2(1-\nu)}. \tag{15}$$

In order to find the displacement, the strain displacement relation $\bar{\varepsilon}_\theta = \bar{u}/\bar{r}$ and Eq. (9) are used. The result is

$$\bar{u} = -\frac{C_1(1+\nu)}{\bar{r}} - \bar{r}C_2(1+\nu)(1-2\nu) - \frac{\bar{r}^3\Omega^2(1+\nu)(1-2\nu)}{8(1-\nu)}. \tag{16}$$

The elastic solution is completed by finding the integration constants C_1 and C_2. For a single tube with traction free surfaces, the boundary conditions read $\bar{\sigma}_{r1}(\bar{a}) = \bar{\sigma}_{r2}(1) = 0$ which give

$$C_1 = -\frac{\bar{a}^2\Omega^2(3-2\nu)}{8(1-\nu)}, \tag{17}$$

$$C_2 = -\frac{(1+\bar{a}^2)\Omega^2(3-2\nu)}{8(1-\nu)}. \tag{18}$$

In the next part, the derivations for the two layer tubes are presented.

2.3 Two Layer Composite Tubes under Rotation

2.3.1 Inner Layer

For the inner layer of the tube, the equilibrium equation in radial direction becomes

$$\frac{d}{dr}(r\sigma_{r1}) - \sigma_{\theta 1} + \rho_1 \omega^2 r^2 = 0, \tag{19}$$

and the generalized Hooke's Law is expressed as

$$\varepsilon_{r1} = \frac{1}{E_1}\left[\sigma_{r1} - \nu_1(\sigma_{\theta 1} + \sigma_{z1})\right], \tag{20}$$

$$\varepsilon_{\theta 1} = \frac{1}{E_1}\left[\sigma_{\theta 1} - \nu_1(\sigma_{r1} + \sigma_{z1})\right], \tag{21}$$

$$\varepsilon_{z1} = \frac{1}{E_1}\left[\sigma_{z1} - \nu_1(\sigma_{r1} + \sigma_{\theta 1})\right]. \tag{22}$$

Using dimensionless and normalized variables

$$\bar{\sigma}_{i1} = \frac{\sigma_{i1}}{\sigma_{01}},\ \Omega^2 = \frac{\omega^2 b^2 \rho_1}{\sigma_{01}},\ \bar{\varepsilon}_{i1} = \frac{\varepsilon_{i1} E_1}{\sigma_{01}}, \tag{23}$$

the dimensionless form of the equilibrium equation in radial direction becomes

$$\frac{d}{d\bar{r}}(\bar{r}\bar{\sigma}_{r1}) - \bar{\sigma}_{\theta 1} + \Omega^2 \bar{r}^2 = 0, \tag{24}$$

and the generalized Hooke's Law will be

$$\bar{\varepsilon}_{r1} = \bar{\sigma}_{r1} - \nu_1(\bar{\sigma}_{\theta 1} + \bar{\sigma}_{z1}), \tag{25}$$

$$\bar{\varepsilon}_{\theta 1} = \bar{\sigma}_{\theta 1} - \nu_1(\bar{\sigma}_{r1} + \bar{\sigma}_{z1}), \tag{26}$$

$$\bar{\varepsilon}_{z1} = \bar{\sigma}_{z1} - \nu_1(\bar{\sigma}_{r1} + \bar{\sigma}_{\theta 1}). \tag{27}$$

Introducing the stress function $Y_1 = \bar{r}\bar{\sigma}_{r1}$, substituting the stress components $\bar{\sigma}_{r1}$ and $\bar{\sigma}_{\theta 1}$ into the equation of equilibrium (24) and using the compatibility relation one obtains

$$\bar{r}^2 \frac{d^2 Y_1}{d\bar{r}^2} + \bar{r}\frac{dY_1}{d\bar{r}} - Y_1 = -\frac{\bar{r}^3\Omega^2(3-2\nu_1)}{1-\nu_1}. \tag{28}$$

Solution of this differential equation for Y_1 gives

$$Y_1 = \frac{C_1}{\bar{r}} + C_2\bar{r} - \frac{\bar{r}^3\Omega^2(3-2\nu_1)}{8(1-\nu_1)}, \tag{29}$$

and the stress components and displacement become

$$\bar{\sigma}_{r1} = \frac{C_1}{\bar{r}^2} + C_2 - \frac{\bar{r}^2\Omega^2(3-2\nu_1)}{8(1-\nu_1)}, \tag{30}$$

$$\bar{\sigma}_{\theta 1} = -\frac{C_1}{\bar{r}^2} + C_2 - \frac{\bar{r}^2\Omega^2(1+2\nu_1)}{8(1-\nu_1)}, \tag{31}$$

$$\bar{\sigma}_{z1} = 2C_2\nu_1 - \frac{\bar{r}^2\Omega^2\nu_1}{2(1-\nu_1)}, \tag{32}$$

$$\bar{u}_1 = -\frac{C_1(1+\nu_1)}{\bar{r}} + \bar{r}C_2(1+\nu_1)(1-2\nu_1) - \frac{\bar{r}^3\Omega^2(1+\nu_1)(1-2\nu_1)}{8(1-\nu_1)}, \tag{33}$$

which are identical with the related expressions obtained for the single tube.

2.3.2 Outer Layer

The procedure applied for the inner layer is used for the outer tube as well. Equilibrium equation in radial direction is

$$\frac{d}{dr}(r\sigma_{r2}) - \sigma_{\theta 2} + \rho_2 \omega^2 r^2 = 0, \tag{34}$$

and the generalized Hooke's Law become

$$\varepsilon_{r2} = \frac{1}{E_2}\left[\sigma_{r2} - \nu_2(\sigma_{\theta 2} + \sigma_{z2})\right], \tag{35}$$

$$\varepsilon_{\theta 2} = \frac{1}{E_2}\left[\sigma_{\theta 2} - \nu_2(\sigma_{r2} + \sigma_{z2})\right], \tag{36}$$

$$\varepsilon_{z2} = \frac{1}{E_2}\left[\sigma_{z2} - \nu_2(\sigma_{r2} + \sigma_{\theta 2})\right], \tag{37}$$

for the outer tube. The dimensionless form of the equilibrium equation can be obtained as

$$\frac{d}{d\bar{r}}(\bar{r}\bar{\sigma}_{r2}) - \bar{\sigma}_{\theta 2} + \Omega^2 \bar{r}^2 \frac{\rho_2}{\rho_1} = 0, \tag{38}$$

Introducing the material ratio $R_2 = \rho_2 / \rho_1$, the equilibrium equation becomes

$$\frac{d}{d\bar{r}}(\bar{r}\bar{\sigma}_{r2}) - \bar{\sigma}_{\theta 2} + \Omega^2 \bar{r}^2 R_2 = 0, \tag{39}$$

and the generalized Hooke's Law can be expressed as

$$\bar{\varepsilon}_{r2} = R_1\left[\bar{\sigma}_{r2} - \nu_2(\bar{\sigma}_{\theta 2} + \bar{\sigma}_{z2})\right], \tag{40}$$

$$\bar{\varepsilon}_{\theta 2} = R_1\left[\bar{\sigma}_{\theta 2} - \nu_2(\bar{\sigma}_{r2} + \bar{\sigma}_{z2})\right], \tag{41}$$

$$\bar{\varepsilon}_{z2} = R_1\left[\bar{\sigma}_{z2} - \nu_2(\bar{\sigma}_{r2} + \bar{\sigma}_{\theta 2})\right], \tag{42}$$

where the material ratio R_1 is defined as

$$R_1 = \frac{E_1}{E_2}. \tag{43}$$

Introducing the stress function $Y_2 = \bar{r}\,\bar{\sigma}_{r2}$, substituting the stress components $\bar{\sigma}_{r2}$ and $\bar{\sigma}_{\theta 2}$ into the equation of equilibrium (39) and using the compatibility relation one finds

$$\bar{r}^2 \frac{d^2 Y_2}{d\bar{r}^2} + \bar{r}\frac{dY_2}{d\bar{r}} - Y_2 = -\frac{\bar{r}^3 \Omega^2 (3-2\nu_2) R_2}{1-\nu_2}. \tag{44}$$

Solution of this differential equation for Y_2 yields

$$Y_2 = \frac{C_3}{\bar{r}} + C_4 \bar{r} - \frac{\bar{r}^3 \Omega^2 R_2 (3-2\nu_2)}{8(1-\nu_2)}, \tag{45}$$

and the stress components and the displacement become

$$\bar{\sigma}_{r2} = \frac{C_3}{\bar{r}^2} + C_4 - \frac{\bar{r}^2 \Omega^2 R_2 (3-2\nu_2)}{8(1-\nu_2)}, \tag{46}$$

$$\bar{\sigma}_{\theta 2} = -\frac{C_3}{\bar{r}^2} + C_4 - \frac{\bar{r}^2 \Omega^2 R_2 (1+2\nu_2)}{8(1-\nu_2)}, \tag{47}$$

$$\bar{\sigma}_{z2} = 2C_4 \nu_2 - \frac{\bar{r}^2 \Omega^2 R_2 \nu_2}{2(1-\nu_2)}, \tag{48}$$

$$\bar{u}_2 = -\frac{C_3 R_1 (1+\nu_2)}{\bar{r}} + \bar{r} C_4 R_1 (1+\nu_2)(1-2\nu_2) - \frac{\bar{r}^3 \Omega^2 R_1 R_2 (1+\nu_2)(1-2\nu_2)}{8(1-\nu_2)}. \tag{49}$$

2.3.3 The Solution

The analytical solution is completed after finding the integration constants C_1, C_2, C_3 and C_4. Since the inner and the outer layers are traction free

$$\overline{\sigma}_{r1}(\overline{a}) = \overline{\sigma}_{r2}(1) = 0\,. \tag{50}$$

In addition, at the interface between the layers, the radial stress components and radial displacements must be continuous and hence one may write

$$\overline{\sigma}_{r1}(\overline{r}_1) = \overline{\sigma}_{r2}(\overline{r}_1)\,, \tag{51}$$

$$\overline{u}_1(\overline{r}_1) = \overline{u}_2(\overline{r}_1)\,. \tag{52}$$

Application of these four non-redundant conditions results in

$$C_1 = -\frac{\overline{a}^2\overline{r}_1^2\Omega^2(D_1D_2D_4(\overline{r}_1^2 - \overline{a}^2D_7) + D_5R_1(D_6D_7(1+D_8\overline{r}_1^2) + 2D_3D_4D_{11}R_2))}{8D_3(D_1D_4(\overline{a}^2 + D_2\overline{r}_1^2) + D_5D_6(1+D_8\overline{r}_1^2)R_1)}, \tag{53}$$

$$C_2 = \frac{\Omega^2(D_1D_4(\overline{a}^4D_7 + D_2\overline{r}_1^4) + D_5R_1(D_7(1+D_8\overline{r}_1^2)(\overline{r}_1^4 - \overline{a}^4) + 2D_3D_4D_{11}\overline{r}_1^2R_2))}{8D_3(D_1D_4(\overline{a}^2 + D_2\overline{r}_1^2) + D_5D_6(1+D_8\overline{r}_1^2)R_1)}, \tag{54}$$

$$C_3 = -\frac{\overline{r}_1^2\Omega^2(2D_1D_6D_9(\overline{a}^2D_7 + D_2\overline{r}_1^2) + R_2(D_4D_{12} - D_6D_{13}R_1(D_9 - 2\nu_2^2)))}{8D_9(D_1D_4(\overline{a}^2 + D_2\overline{r}_1^2) + D_5D_6(1+D_8\overline{r}_1^2)R_1)}, \tag{55}$$

$$C_4 = \frac{\Omega^2(2D_1D_6D_9\overline{r}_1^2(\overline{a}^2D_7 + D_2\overline{r}_1^2) + R_2(D_{12} - D_{12}\overline{r}_1^4 + D_5D_6R_1(3 + D_8\overline{r}_1^4 - 2\nu_2)))}{8D_9(D_1D_4(\overline{a}^2 + D_2\overline{r}_1^2) + D_5D_6(1+D_8\overline{r}_1^2)R_1)}, \tag{56}$$

where

$$D_1 = 1 + \nu_1, \tag{57}$$

$$D_2 = 1 - 2\nu_1, \tag{58}$$

$$D_3 = 1 - \nu_1, \tag{59}$$

$$D_4 = 1 - \bar{r}_1^2, \tag{60}$$

$$D_5 = 1 + \nu_2, \tag{61}$$

$$D_6 = \bar{r}_1^2 - \bar{a}^2, \tag{62}$$

$$D_7 = 3 - 2\nu_1, \tag{63}$$

$$D_8 = 1 - 2\nu_2, \tag{64}$$

$$D_9 = 1 - \nu_2, \tag{65}$$

$$D_{10} = 3 - 2\nu_2, \tag{66}$$

$$D_{11} = 3 + \bar{r}_1^2 - 2(1 + \bar{r}_1^2)\nu_2, \tag{67}$$

$$D_{12} = D_1 D_{10}(\bar{a}^2 + D_2 \bar{r}_1^2), \tag{68}$$

$$D_{13} = D_{10} - \bar{r}_1^2. \tag{69}$$

2.4 Yielding of the Two-Layer Tubes

Since the analytical solutions are obtained, the yielding behaviour can be studied. The von Mises yield criterion [3] in a cylindrical coordinate system can be expressed as

$$\sigma_Y = \sqrt{\frac{1}{2}[(\sigma_r - \sigma_\theta)^2 + (\sigma_r - \sigma_z)^2 + (\sigma_\theta - \sigma_z)^2]}. \tag{70}$$

Here σ_Y is the von Mises yield stress. If $\sigma_Y = \sigma_0$, yielding begins and for the cases where $\sigma_Y < \sigma_0$ the shaft is in elastic stress state. It is known that for a single layer

rotating tube, yielding commences at the inner surface according to von Mises criterion and the elastic limit angular velocity $\Omega = \Omega_e$ is given as [8]

$$\Omega_e = \sqrt{\frac{4(1-\nu)}{(3-2\nu+\bar{a}^2(1-2\nu))\sqrt{(1-\nu(1-\nu))}}} \quad . \tag{71}$$

Studies showed that in a two-layer tube, yielding may begin at the inner surface of the inner tube ($\bar{r} = \bar{a}$) or at the inner surface of the outer tube ($\bar{r} = \bar{r}_1$). In order to monitor the yielding behaviour at the inner tube, the nondimensional stress variable ϕ_1 for the inner surface (at $\bar{r} = \bar{a}$) is introduced as

$$\phi_1 = \sqrt{\frac{1}{2}[(\bar{\sigma}_{r1}(\bar{a}) - \bar{\sigma}_{\theta 1}(\bar{a}))^2 + (\bar{\sigma}_{r1}(\bar{a}) - \bar{\sigma}_{z1}(\bar{a}))^2 + (\bar{\sigma}_{\theta 1}(\bar{a}) - \bar{\sigma}_{z1}(\bar{a}))^2]}\,. \tag{72}$$

The yielding occurs as soon as $\phi_1 = 1$ and for $\phi_1 < 1$ the inner tube is in elastic stress state. Similarly, for the outer tube, the stress variable ϕ_2 at $\bar{r} = \bar{r}_1$ is defined as

$$\phi_2 = \sqrt{\frac{1}{2}[(\bar{\sigma}_{r2}(\bar{r}_1) - \bar{\sigma}_{\theta 2}(\bar{r}_1))^2 + (\bar{\sigma}_{r2}(\bar{r}_1) - \bar{\sigma}_{z2}(\bar{r}_1))^2 + (\bar{\sigma}_{\theta 2}(\bar{r}_1) - \bar{\sigma}_{z2}(\bar{r}_1))^2]}\,. \tag{73}$$

In this case, the yielding occurs at $\phi_2 = 1$ and for $\phi_2 < 1$ the outer tube is in elastic stress state. Using these equations, the commencement of the yielding of the tubes can be monitored and the corresponding elastic limit angular velocities can be evaluated.

Different from these two yielding behaviours, as a special case, the yielding may commence at the inner surfaces of both layers simultaneously. Finding the critical parameters for this case requires considering the onset of yield at both locations $\bar{r} = \bar{a}$ and $\bar{r} = \bar{r}_1$. The numerical solution of the equations (72) and (73) simultaneously for the dimensionless elastic limit angular speed Ω_e and the critical interface radius $(\bar{r}_1)_{cr}$ gives the pair that cause yielding at the inner surface and at the interface at the same time. For this case, it is also found that for the interface diameter $\bar{r}_1 > (\bar{r}_1)_{cr}$, yielding begins at the inner surface $\bar{r} = \bar{a}$ and for the values

$\bar{r}_1 < (\bar{r}_1)_{cr}$ yielding commences at the interface $\bar{r} = \bar{r}_1$. In order to clarify this special case and the other cases presented above, several examples are handled in the next part.

CHAPTER III

NUMERICAL RESULTS

3.1 General

The analytical solution of the rotating two-layer composite tube problem was presented in Chapter II. In this chapter, some numerical results containing the stresses and displacements that are derived in the previous chapter will be given. In the following parts, the yielding behaviour of a single tube is presented first. Then, the yielding of the two-layer tube assembly will be analysed. For the presentation of the numerical results of the composite tubes, several combinations of aluminium, brass, copper and steel are used. The material properties which are used in the computations are given in Table 3.1. In addition to the stress and displacement distributions, for each composite tube, the dimensional displacement versus dimensional angular velocity at the interface of the two separate tubes (inner tube: from a to r_i, outer tube: from r_i to b) will be given in order to check the validity of the interface conditions.

Table 3.1. Mechanical properties of the materials used in the numerical results

	E (GPa)	ν	σ_o (MPa)	ρ (kg/m^3)
Aluminium	70	0.35	100	2700
Brass	105	0.35	410	8470
Copper	120	0.365	265	8910
Steel	200	0.30	430	7800

3.2 Single Tube Results

As stated previously, for a single tube, yielding begins at the inner surface. Considering an aluminium tube and taking $\bar{a} = a/b = 0.7$, the elastic limit angular velocity is obtained as $\Omega_e = 1.09950$ using Eq. (71). With the help of Eqs. (17) and (18) the integration constants are determined as $C_1 = -0.262006$ and $C_2 = 0.796711$. Figure 3.1 presents the corresponding stresses and displacement. It is noted that the stress variable $\phi = 1$ at $\bar{r} = \bar{a}$.

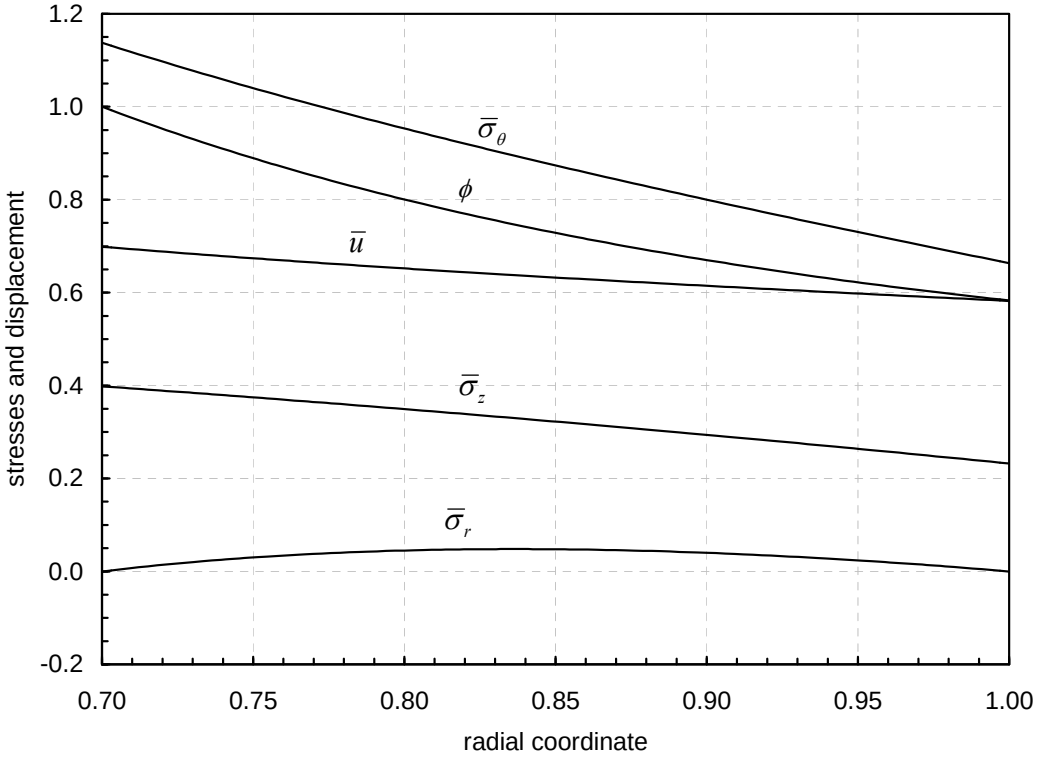

Figure 3.1 The distributions of stresses and displacement in a rotating aluminium tube ($\bar{a} = 0.7$) **at** $\Omega_e = 1.09950$.

For a brass tube with $\overline{a} = 0.4$, Eq. (71) gives $\Omega_e = 1.12244$. The corresponding integration constants are obtained as $C_1 = -0.891601 \times 10^{-1}$ and $C_2 = 0.646411$ using Eqs. (17) and (18). The consequent stresses and displacement are given in Figure 3.2.

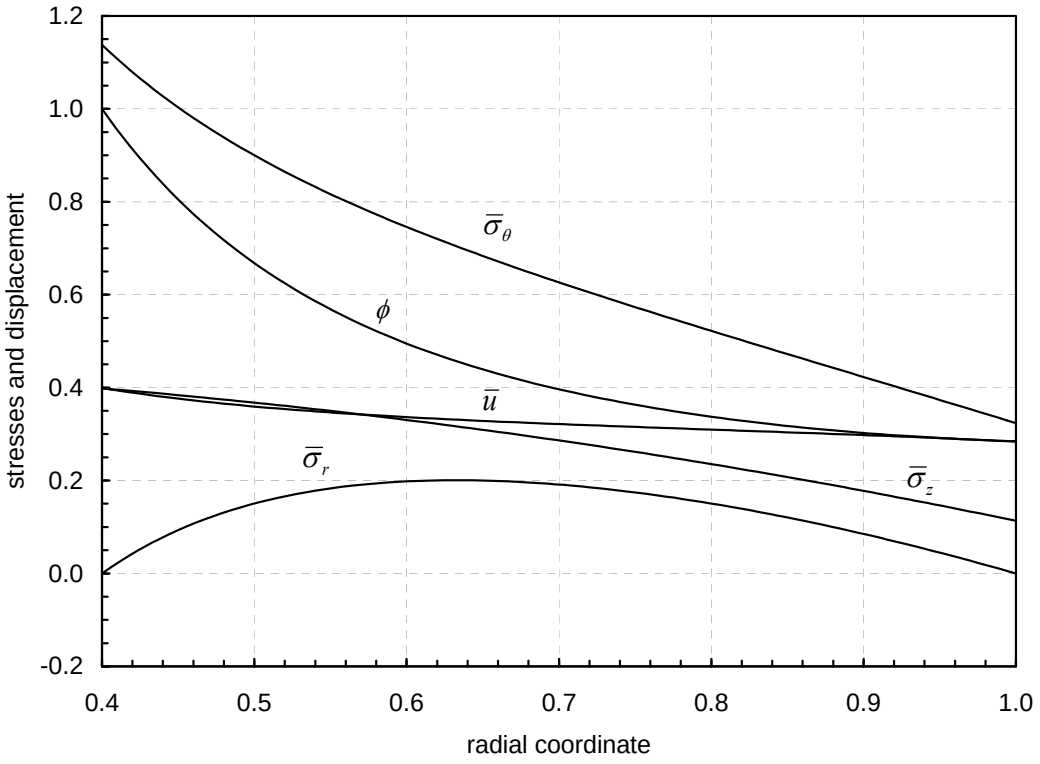

Figure 3.2 The distributions of stresses and displacement in a rotating brass tube ($\overline{a} = 0.4$) at $\Omega_e = 1.12244$.

A copper tube with $\overline{a} = 0.7$ yields at $\Omega_e = 1.09833$. The integration constants are calculated as $C_1 = -0.264132$ and $C_2 = 0.803176$, and in Figure 3.3 the corresponding distributions of the stresses and displacement are shown.

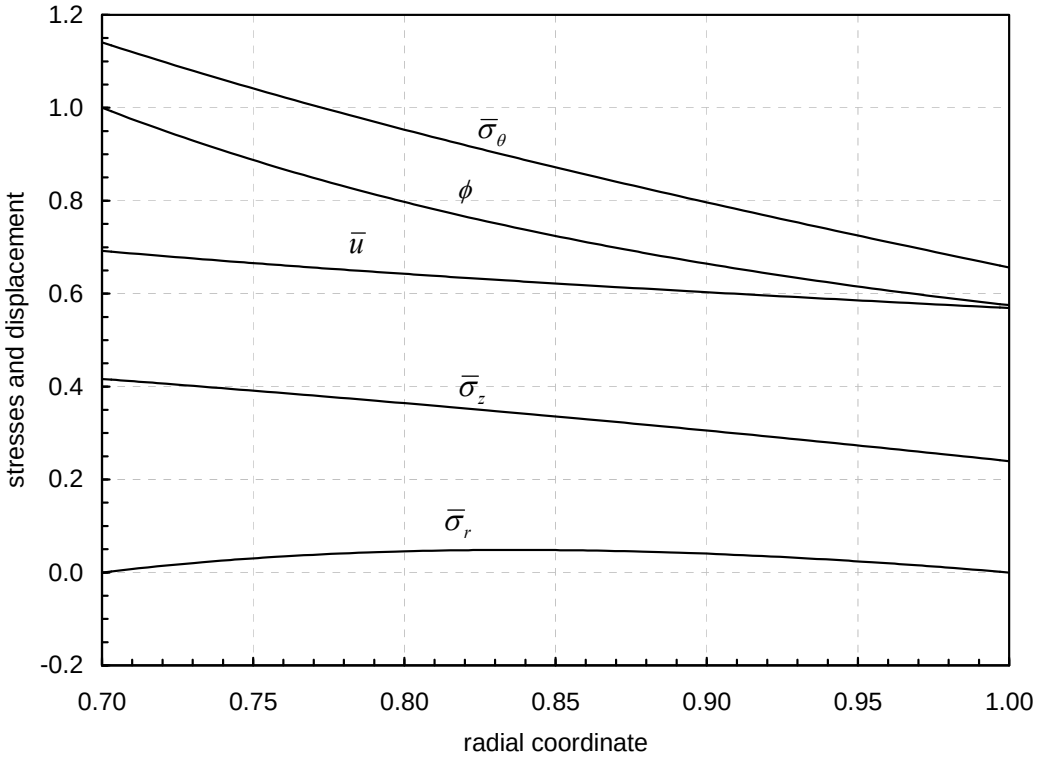

Figure 3.3 The distributions of stresses and displacement in a rotating copper tube ($\overline{a} = 0.7$) at $\Omega_e = 1.09833$.

Finally, as a last example, for a steel tube with $\overline{a} = 0.8$, yielding begins at the elastic limit angular velocity $\Omega_e = 1.08908$. The corresponding integration constants are obtained as $C_1 = -0.325327$ and $C_2 = 0.833649$. The corresponding stresses and displacement are shown in Figure 3.4.

In the next part, the results obtained for the two layer rotating tubes are presented.

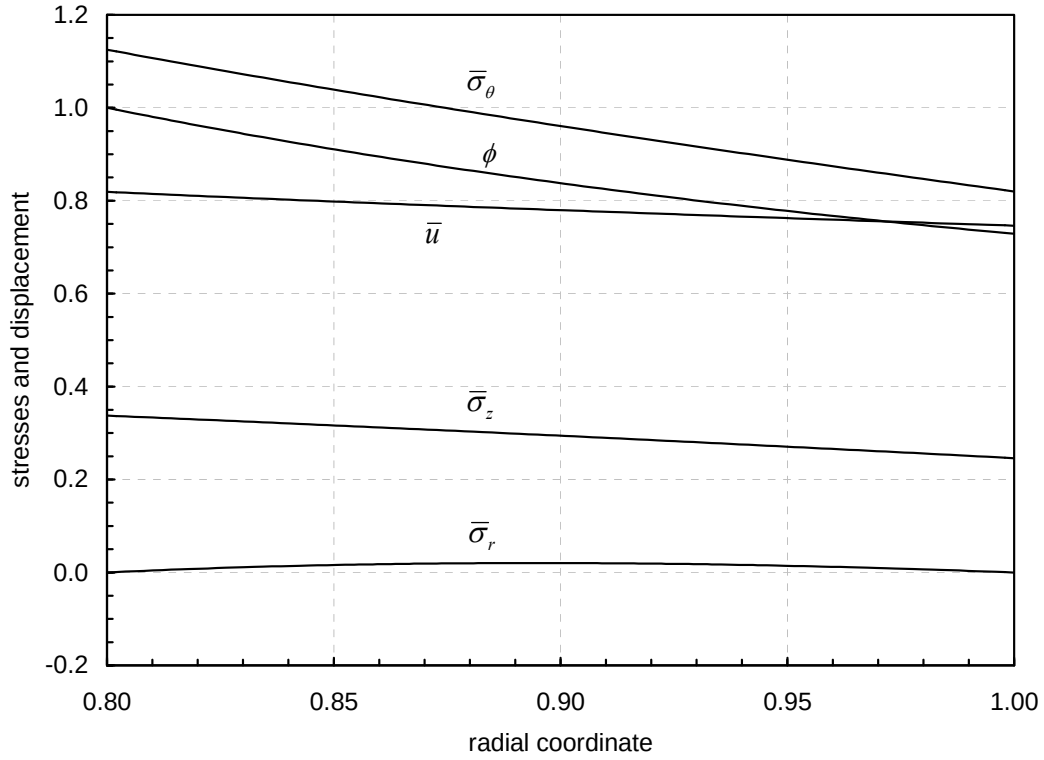

Figure 3.4 The distributions of stresses and displacement in a rotating steel tube ($\bar{a} = 0.8$) at $\Omega_e = 1.08908$.

3.3 Two Layer Tube Results

In order to clarify the yielding behaviour of the rotating two-layer tubes, several geometries are investigated. Among different combinations of the materials (brass, copper, aluminium and steel), suitable pairs that satisfy the interface condition $\bar{u}_1(\bar{r}_1) = \bar{u}_2(\bar{r}_1)$ are considered. Since the tubes are tightly fitted, interface displacements must be checked in order to ensure that the connection between the layers is not lost for the given set of materials at the determined velocities. In order to check this condition, the two tubes are separated from each other (inner tube: from a to r_1, outer tube: from r_1 to b) and rotated with the same angular velocity where the single tube relations are valid. Then, the dimensional displacement of the outer surface of the inner tube is compared with the dimensional displacement of the inner

surface of the outer tube for the rotation speeds up to the elastic limit velocity. If the displacement $u_2(r_1)$ is less than the displacement $u_1(r_1)$ for the separate tubes, the interface condition stated above is satisfied. This procedure is performed for all composite tubes that are investigated.

For the cases where inner layer is brass and the outer layer is steel or aluminium, the yielding is observed to begin at the interface first. For example, for a brass-aluminium composite tube with $\bar{a} = 0.7$ and $\bar{r}_1 = 0.85$, yielding begins at the aluminium tube. The elastic limit angular velocity is calculated as $\Omega_e = 0.910622$ by the numerical solution of the Eq. (73) for $\phi_2 = 1$. The corresponding integration constants are obtained as $C_1 = -0.125241$, $C_2 = 0.435314$, $C_3 = -0.923502 \times 10^{-1}$ and $C_4 = 0.209268$ using Eqs. (53)-(56). Figure 3.5 shows the consequent stresses and displacement.

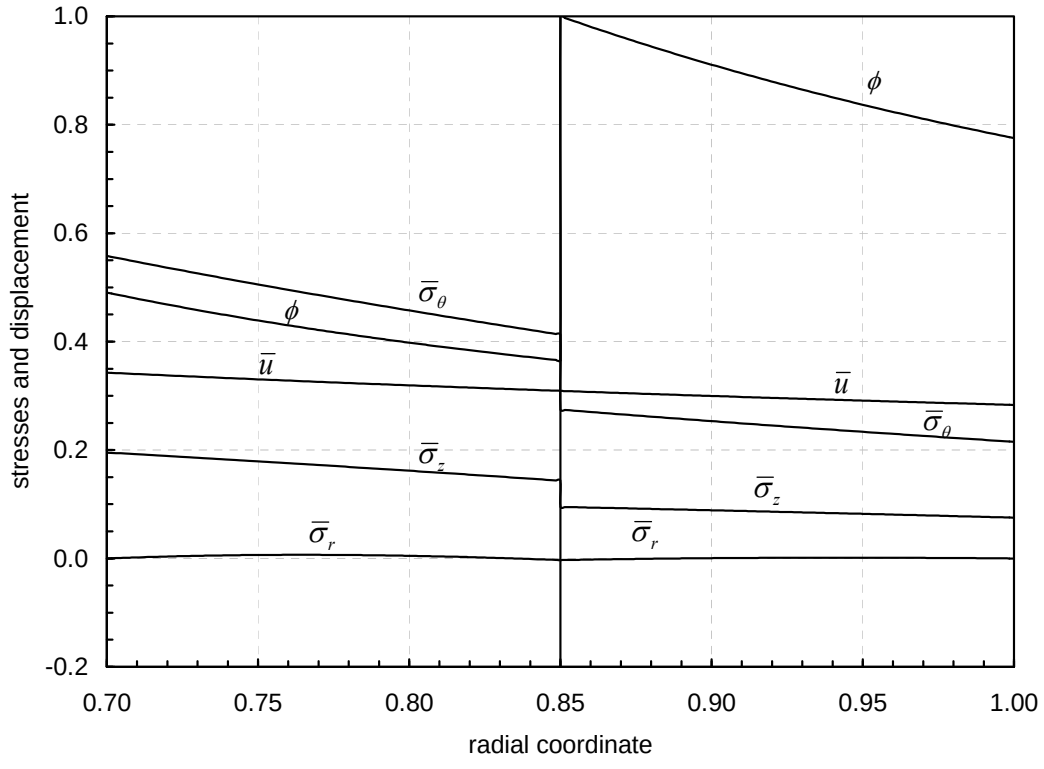

Figure 3.5 The distributions of stresses and displacement in a rotating brass-aluminium composite tube ($\bar{a} = 0.7, \bar{r}_1 = 0.85$) at $\Omega_e = 0.910622$.

It should be noted that at $\bar{r}_1 = 0.85$ the yield variable $\phi = 1$, while it is smaller than one in all other locations. This situation implies the commencement of the yielding at the aluminium outer tube where $\bar{r} = \bar{r}_1$. It should also be stated that the boundary and the interface conditions that are given in the Eqs. (50), (51) and (52) are perfectly satisfied. In addition to these, the dimensional interface displacement versus dimensional angular velocity curves of the separated brass ($a = 0.7, b = 0.85$) and aluminium ($a = 0.85, b = 1.0$) tubes are given in Figure 3.6. It is shown in this figure that $u_2(r_1)$ is always less than $u_1(r_1)$ for all rotation speeds up to the dimensional elastic limit angular velocity $\omega = 209.952$ rad/s , which implies the correctness of the solution.

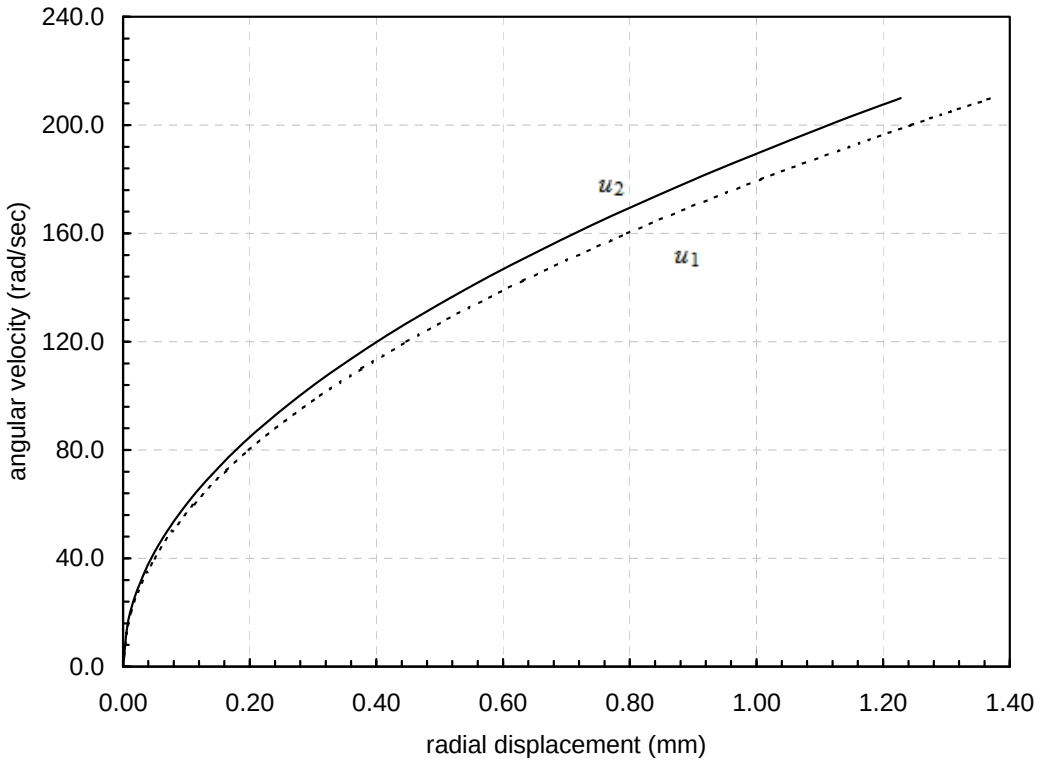

Figure 3.6 The dimensional inner and outer tube displacements at r_1 with respect to the angular velocity for the brass-aluminium tube ($\bar{a} = 0.7, \bar{r}_1 = 0.85$).

Steel outer layer with the interface radius $\bar{r}_1 = 0.85$ also yields before the brass inner layer at $\Omega_e = 1.13580$. The corresponding integration constants are calculated using equations (53)-(56) as $C_1 = -0.193634$, $C_2 = 0.674764$, $C_3 = -0.382169$ and $C_4 = 0.891311$. The resulting stresses and displacement are shown in Figure 3.7 and the check for the interface displacement is made in Figure 3.8. It is again observed that at the interface, the stress variable is $\phi = 1$ which shows the beginning of yielding at the outer tube.

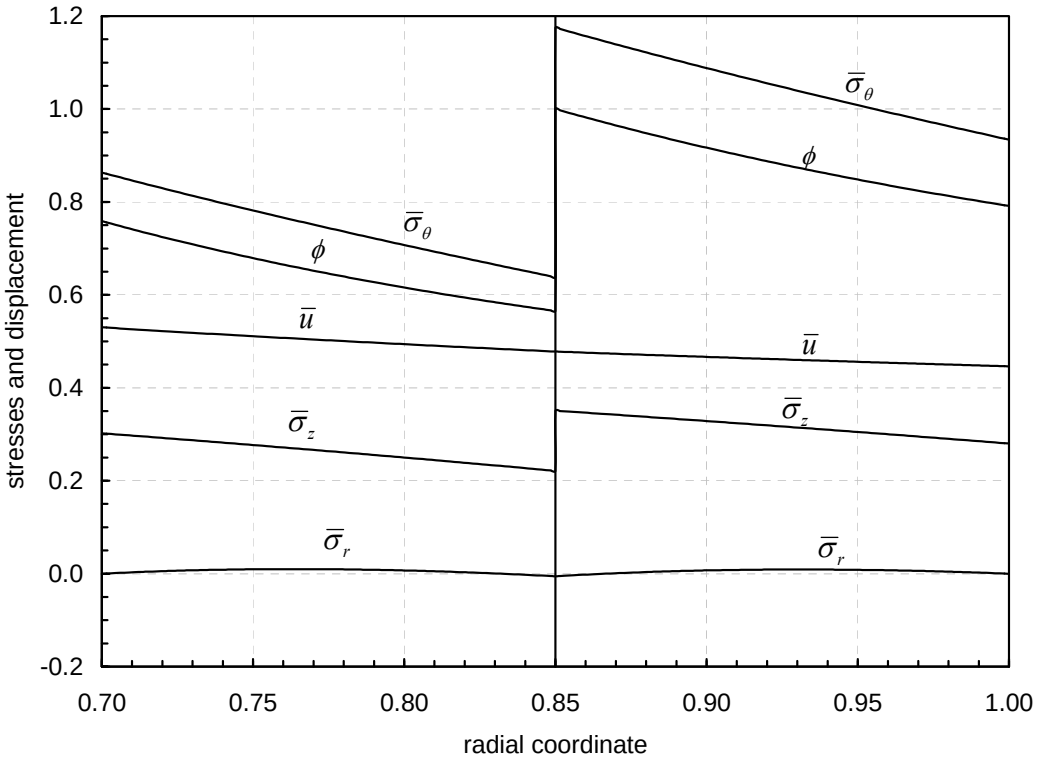

Figure 3.7 The distributions of stresses and displacement in a rotating brass-steel composite tube ($\bar{a} = 0.7, \bar{r}_1 = 0.85$) at $\Omega_e = 1.13580$.

In the case of copper inner layer and steel the outer layer, choosing the inner radius as $\bar{a} = 0.75$ and the interface radius as $\bar{r}_1 = 0.85$, yielding begins in the inner surface

of the copper layer. For this case the elastic limit angular velocity is obtained as $\Omega_e = 1.30812$ by the numerical solution of Eq. (72) for $\phi_1 = 1$. The corresponding integration constants are calculated using equations (53)-(56) as $C_1 = -0.292108$, $C_2 = 0.949413$, $C_3 = -0.482959$ and $C_4 = 0.112496 \times 10^1$. The resulting stresses and displacement are shown in Figure 3.9 and in Figure 3.10 the interface displacements for the two separate tubes are given up to the dimensional elastic limit angular velocity ($\omega = 197.246$) of the composite tube.

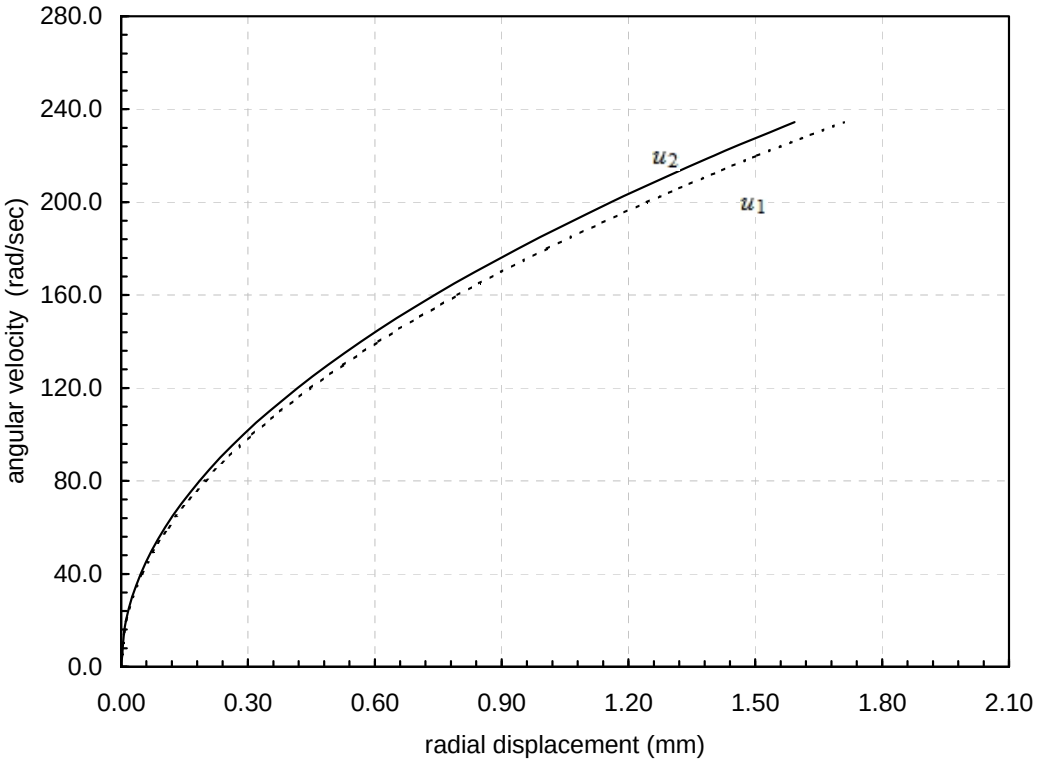

Figure 3.8 The dimensional inner and outer tube displacements at r_1 with respect to the angular velocity for the brass-steel tube ($\bar{a} = 0.7$, $\bar{r}_1 = 0.85$).

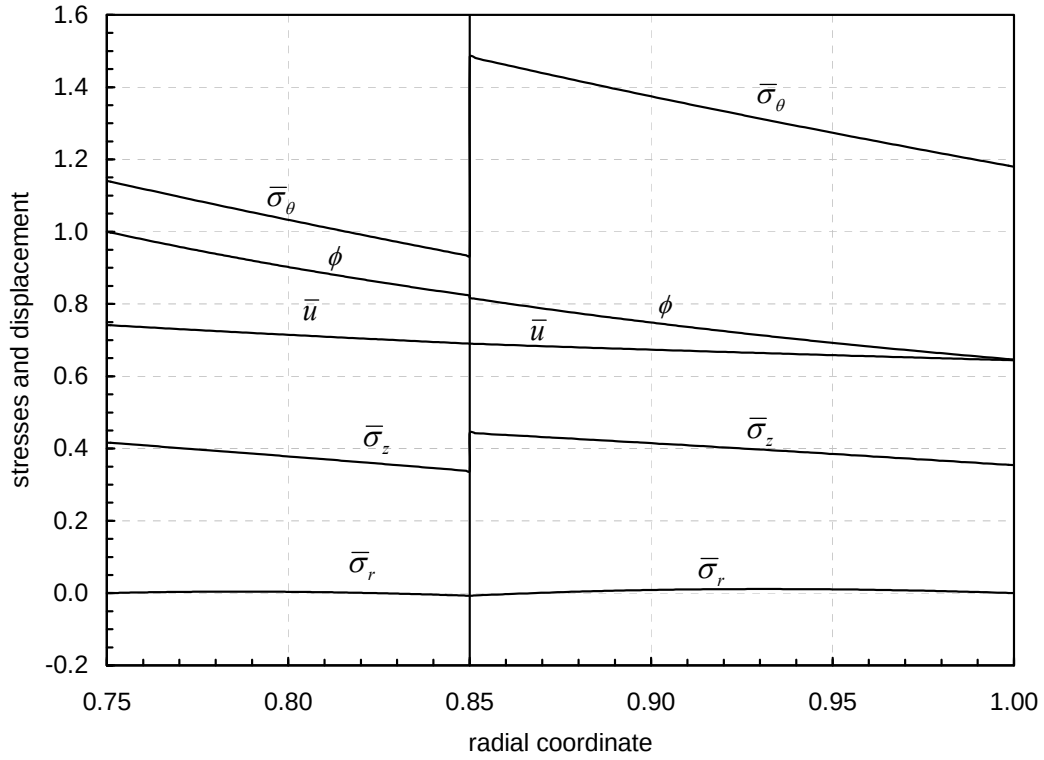

Figure 3.9 The distributions of stresses and displacement in a rotating copper-steel composite tube ($\overline{a} = 0.75$, $\overline{r}_1 = 0.85$) at $\Omega_e = 1.30812$.

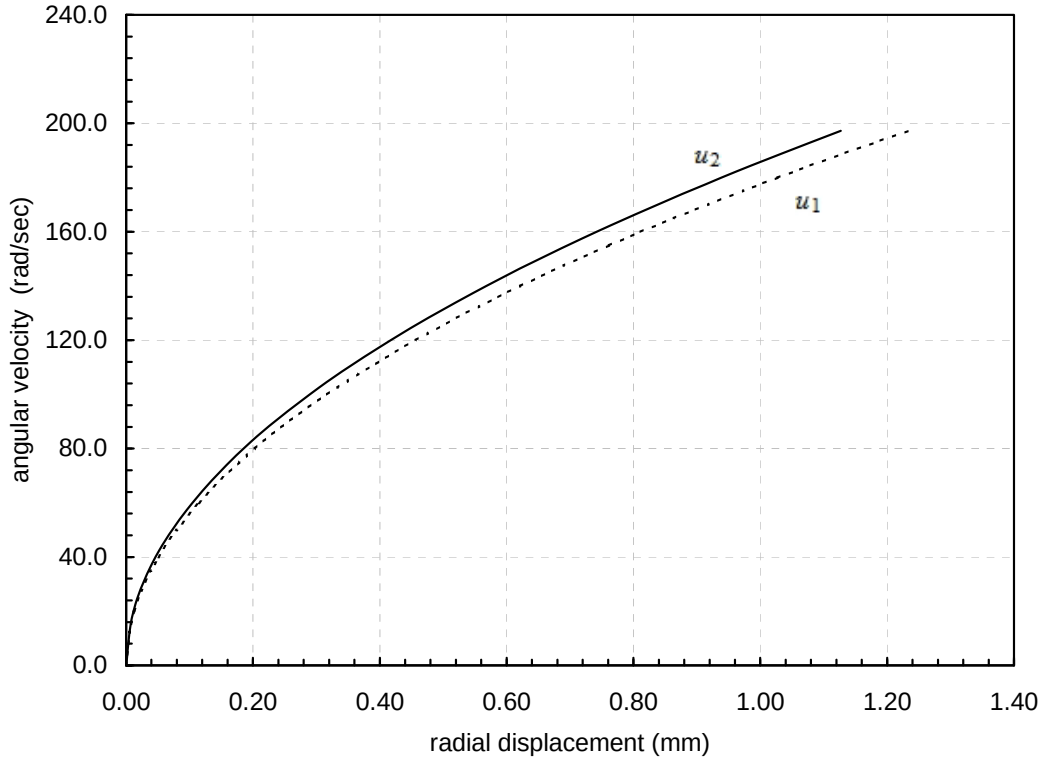

Figure 3.10 The dimensional inner and outer tube displacements at r_1 with respect to the angular velocity for the copper-steel tube ($\bar{a} = 0.75$, $\bar{r}_1 = 0.85$)

Theoretically for any set of elements, there may exist several possibilities of $\bar{a}$, $\bar{r}_1$, and Ω_e values which lead the yielding of one of the layers (inner or outer) first or yielding of both layers simultaneously. Therefore, the examining of a critical interface radius $(\bar{r}_1)_{cr}$ and a corresponding elastic limit angular velocity Ω_e for which the plastic flow begins simultaneously at both $\bar{r} = \bar{a}$ and $\bar{r}_1 = (\bar{r}_1)_{cr}$ becomes critical. However, the first step is finding an elastic limit angular velocity satisfying the Eqs. (72) and (73) separately (for $\phi_1 = 1$ and $\phi_2 = 1$), for a selected $\bar{r}_1$ value. In this special case, to check the possibility of yielding at inner surfaces of both layers simultaneously, a significant number of trials are performed for finding a suitable material combination. The equations are solved simultaneously by Newton iterations in order to find the critical parameters $(\bar{r}_1)_{cr}$ and Ω_e. On the other hand, the interface

displacements for the separate inner and outer tubes are also checked for these parameters. Among several material pairs formed, only using a copper-aluminium pair gave consistent results.

As an example for this special case, when the copper inner layer with $\bar{a} = 0.7$ is combined with the aluminium outer layer, yielding begin at inner surface, at the interface or at both simultaneously for different interface coordinates. The results for these cases are summarized below.

By solving the equations (72) and (73) for $\phi_1 = 1$ and $\phi_2 = 1$ using Newton iterations, the critical parameters are obtained as $(\bar{r}_1)_{cr} = 0.920155$ and $\Omega_e = 1.18930$. The corresponding integration constants are calculated using equations (53)-(56) as $C_1 = -0.261476$, $C_2 = 0.843326$, $C_3 = -0.164048$ and $C_4 = 0.353630$. The resulting stresses and displacements are shown in Figure 3.11.

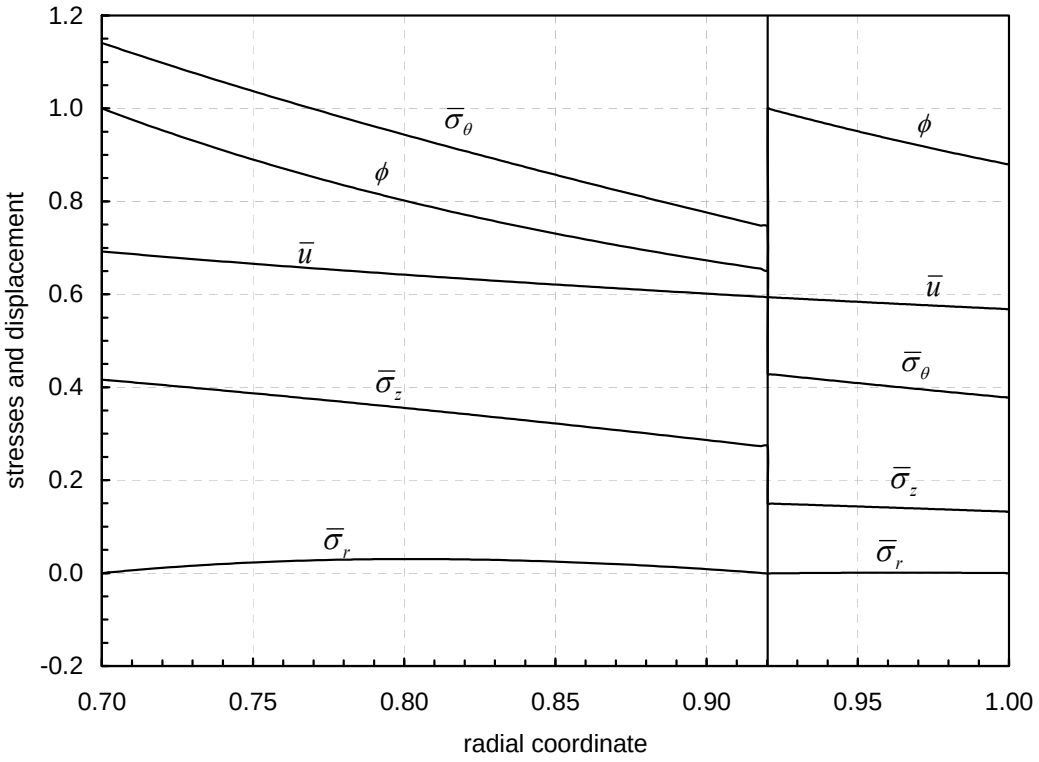

Figure 3.11 The distributions of stresses and displacement in a rotating copper-aluminium composite tube ($\bar{a} = 0.7$, $(\bar{r}_1)_{cr} = 0.920155$) at $\Omega_e = 1.18930$.

It is seen from the figure that the boundary and continuity conditions are fully satisfied for this data set. In addition, the stress variable is 1 at the inner surface and at the interface of the tube assembly. The corresponding dimensional interface displacements for the separate tubes up to the elastic limit angular velocity $\omega = 188.074$ are given in Figure 3.12.

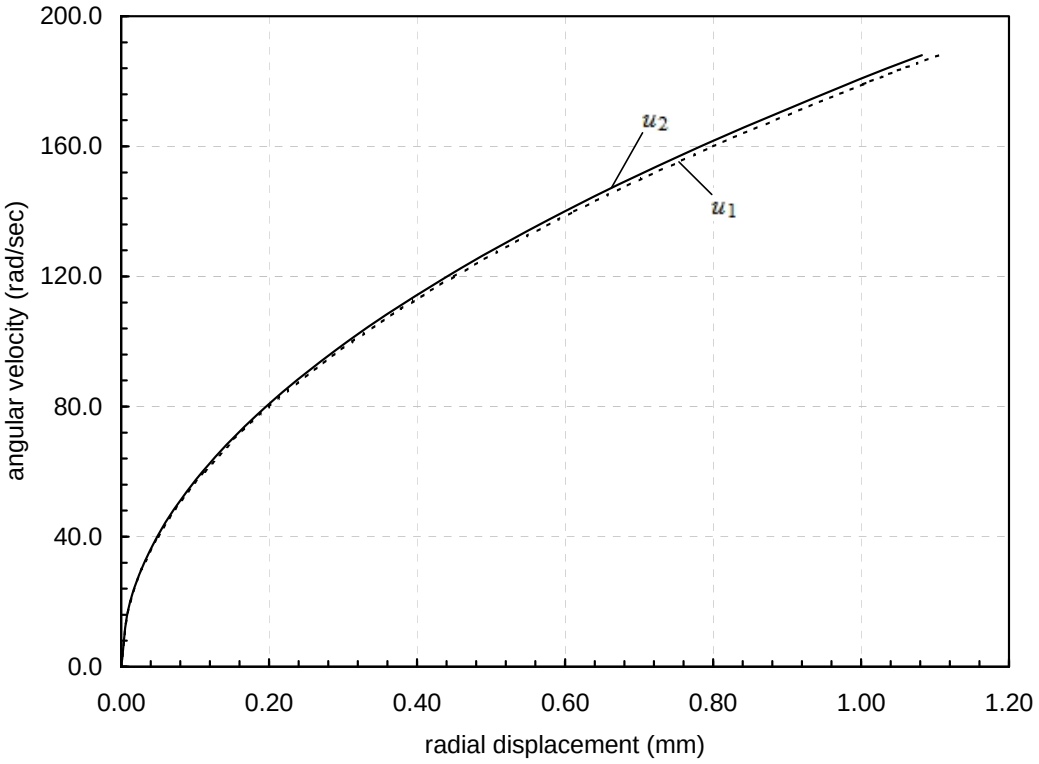

Figure 3.12 The inner and outer tube displacements at $(\bar{r}_1)_{cr}$ with respect to angular velocity for copper-aluminium tube ($\bar{a} = 0.7$, $(\bar{r}_1)_{cr} = 0.920909$).

Since the critical interface coordinate that cause yielding is obtained, the conditions for the yielding at the inner surface and at the interface are considered next. In order to serve this purpose two different interface values are selected. As stated in the previous chapter, for the interface diameter $\bar{r}_1 > (\bar{r}_1)_{cr}$, yielding begins at the inner

surface $\bar{r} = \bar{a}$ and for the values $\bar{r}_1 < (\bar{r}_1)_{cr}$ yielding commences at the interface $\bar{r} = \bar{r}_1$.

Firstly, taking $\bar{r}_1 = 0.85 < (\bar{r}_1)_{cr}$ the elastic limit angular velocity is obtained as $\Omega_e = 1.20478$ by the solution of Eq. (73) for $\phi_2 = 1$. The corresponding integration constants are calculated as $C_1 = -0.228856$, $C_2 = 0.784865$, $C_3 = -0.141865$ and $C_4 = 0.336411$ using equations (53)-(56). The resulting stresses and displacements are shown in Figure 3.13. In this figure, dimensional stress variable ϕ is 1 at $\bar{r}_1 = 0.85$ which implies the yielding at the interface. In Figure 3.14 the interface displacements for the two separate tubes are given.

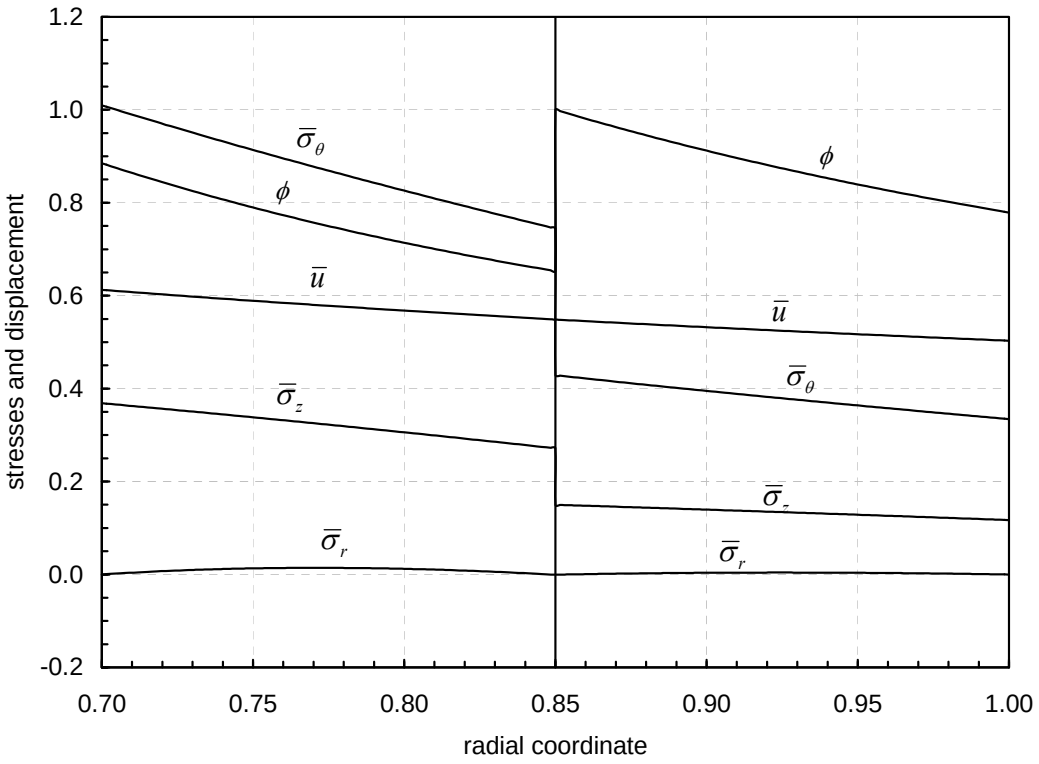

Figure 3.13 The distributions of stresses and displacement in a rotating copper-aluminium composite tube ($\bar{a} = 0.7$, $\bar{r}_1 = 0.85$) at $\Omega_e = 1.20478$.

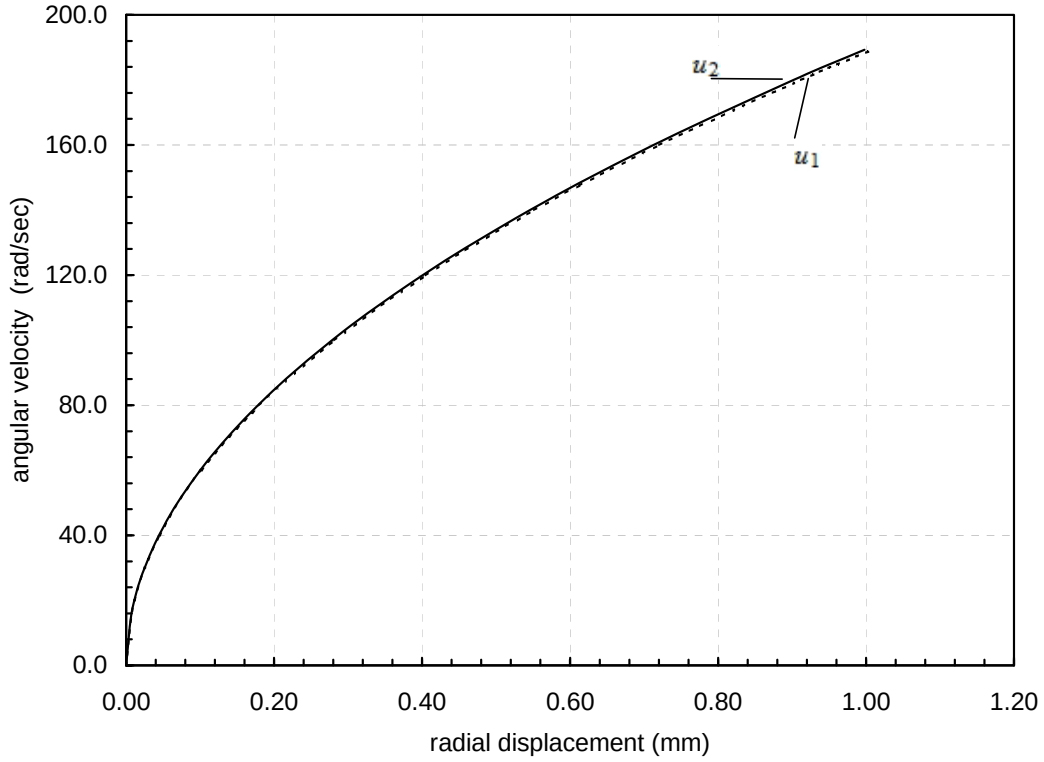

Figure 3.14 The dimensional inner and outer tube displacements at $\bar{r}_1$ with respect to the angular velocity copper-aluminium tube ($\bar{a} = 0.7$, $\bar{r}_1 = 0.85$).

Finally, for $\bar{r}_1 = 0.95 > (\bar{r}_1)_{cr}$, the elastic limit angular velocity is obtained as $\Omega_e = 1.15379$ by the solution of Eq. (72) for $\phi = 1$. The integration constants are calculated as $C_1 = -0.262538$, $C_2 = 0.827274$, $C_3 = -0.165573$ and $C_4 = 0.344003$. The resulting stresses and displacements are shown in Figure 3.15. As seen in this figure, dimensional stress variable ϕ is 1 at $\bar{a} = 0.7$ which implies yielding at the inner surface of the assembly. The interface displacements for the two separate tubes are given in Figure 3.16. It is observed from this figure that at any given angular velocity, at the interface the displacement of inner tube is greater than the displacement of outer tube.

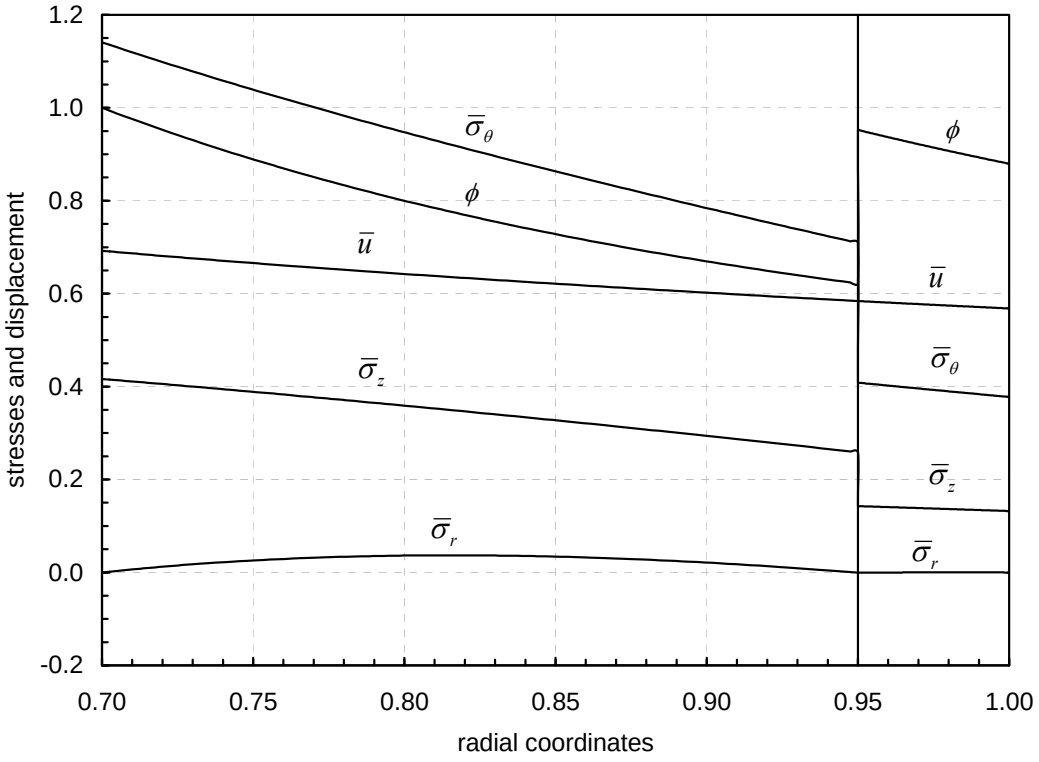

Figure 3.15 The distributions of stresses and displacement in a rotating copper-aluminium composite tube ($\overline{a} = 0.7,\ \overline{r}_1 = 0.95$) at $\Omega_e = 1.15379$.

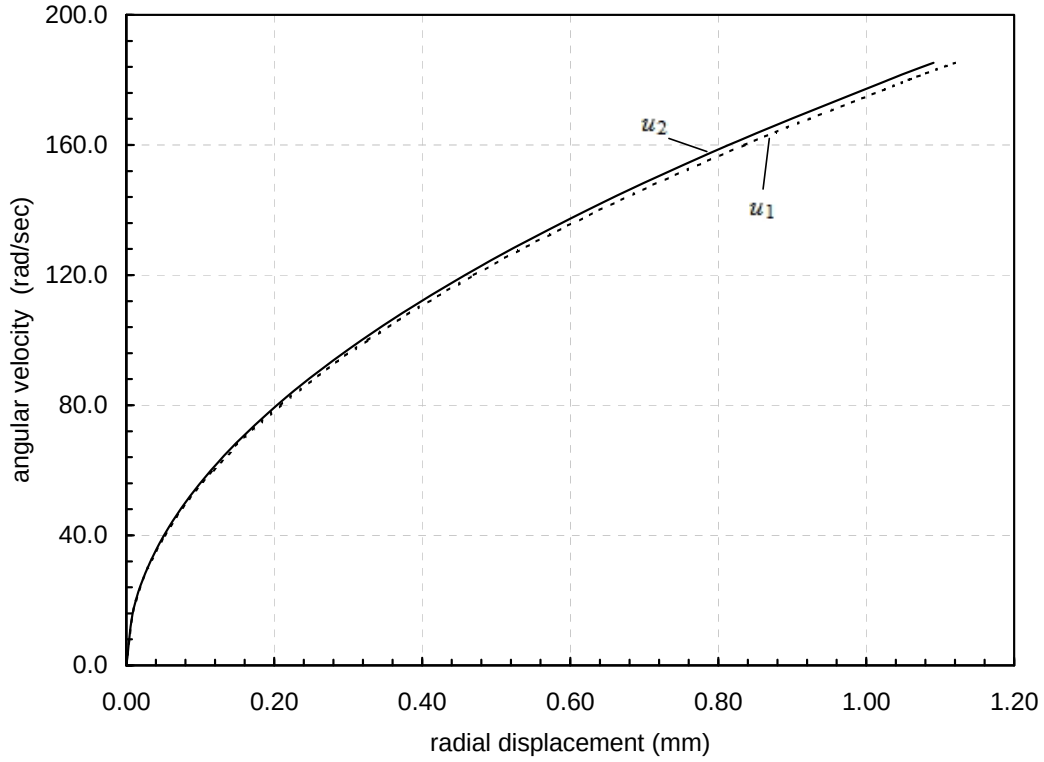

Figure 3.16 The dimensional inner and outer tube displacements at $\bar{r}_1$ with respect to the angular velocity copper-aluminium tube ($\bar{a} = 0.7$, $\bar{r}_1 = 0.95$).

CHAPTER IV

SUMMARY AND CONCLUSION

In this study, the analytical solution of a two-layer composite tube under rotation is presented. Starting with a single tube, the expressions of the stresses and displacement for the tube assembly are derived. Using these expressions, for a selected set of materials, several numerical examples are handled in order to show the yielding behaviour of the tubes. In the study, von Mises yield criterion is used to determine the commencement of the plastic flow in the composite tubes.

In view of the results gathered during this study, three different yielding conditions are found:

1. Yielding at the inner surface of the assembly ($\bar{r} = \bar{a}$) first.
2. Yielding at the interface of the two tubes ($\bar{r} = \bar{r}_1$) first.
3. Yielding simultaneously at both locations $\bar{r} = \bar{a}$ and $\bar{r} = \bar{r}_1$.

The starting of the plastic flow is monitored by considering the Von Mises' yield criterion for the inner and outer layers separately. The elastic limit angular velocities, which cause yielding at the locations stated above, are also determined by the numerical solution of the equations obtained by using the yield criterion.

In addition to the studies performed on the yielding behaviour, the considered tubes with the selected material sets are checked for the validity of the interface conditions by considering the assembly as two separate tubes.

Studies showed that, for the brass-steel and brass-aluminium tubes, the yielding always begins at the inner surface of the outer layer before the inner layer starts to yield. Conversely, for the copper-steel tube, yielding begins at the inner surface of the inner tube. The case for which the yielding starts simultaneously at the inner surfaces of both layers is obtained only for the copper-aluminium tube assembly as the boundary conditions are satisfied only for this set, This geometry is examined further and it is observed that by shifting the interface radius, the location of the yielding may vary. It may yield at the inner surface or at the interface first. Although the material properties are important, for this case, the yielding mainly depends on the thickness of the layers, in other words, the inner radius and the interface radius. For the tube geometry defined, shifting the interface radius outwards, the yielding begins at the interface only until the critical radius $(\bar{r}_1)_{cr}$ is reached. Shifting the interface further the yielding starts to begin at inner radius only. For each case, from the inner to outer radius, the elastic limit angular velocities may change, yet the defined behaviour remains the same. In other words, for the interface diameter $\bar{r}_1 > (\bar{r}_1)_{cr}$, yielding begins at the inner surface $\bar{r} = \bar{a}$ and for the values $\bar{r}_1 < (\bar{r}_1)_{cr}$ yielding begins at the interface $\bar{r} = \bar{r}_1$.

The numerical results reveal that, in the determination of the yielding behaviour for any composite system, main problem lies in satisfying the boundary conditions. Especially, continuity at interface can not be satisfied easily since the tubes are assumed to be tightly fitted and are not fixed to each other by any means. The problem rose from this condition is that at the higher rotation speeds, the outer layer displacement at interface may be greater than the inner layer displacement at the interface. When this happens, in other words, when the tubes lose contact at the interface, the boundary conditions are no longer valid; therefore the problem looses validity as well. Since, the tightly fitted tube may be regarded as a theoretical concept, this behaviour may be expected and appropriate sets of materials are selected among many possibilities by trial. In the study, the numerical results are

generated only for these sets, for which the interface conditions are numerically valid.

For the future studies, this study may be used to develop analytical solutions for the rotating two-layer tubes under different boundary and interface conditions. For instance, the combination of the tubes by shrink fit methods can be examined and the necessary conditions to reach the predetermined yielding behaviour and shrink fit displacement to be applied can be determined. Also, the presence of inner or outer pressure can be added to the problem as a study on a possible practical case.

REFERENCES

[1] Timoshenko S.P., Goodier J.N., Theory of Elasticity, 3rd Ed., McGraw-Hill, New York, 1970.

[2] Timoshenko, S.P., Strength of Materials: Part II Advanced Theory and Problems, 3rd Edition, D. van Nostrand Company, New York, 1956.

[3] Da Silva V.D., Mechanics and Strength of Materials, Springer-Verlag, Berlin Heidelberg, 2006.

[4] Gamer U., Lance R.H., Stress Distribution in a Rotating Elastic-Plastic Tube, Acta Mechanica 50, 1–8, 1983.

[5] Mack W., Rotating Elastic-Plastic Tube with Free Ends, International Journal of Solids Structures, Vol. 27, No. 11, 1461–1476, 1991.

[6] Mack W., The Rotating Elastic-Plastic Solid Shaft with Free Ends, Technische Mechanik 12, 119–124, 1991.

[7] Gamer, U., Mack, W., Varga, I., Rotating Elastic-Plastic Solid Shaft with Fixed Ends, International Journal of Engineering Sciences, Vol.35, No. 3, 253-267,1997.

[8] Eraslan A.N., Von Mises' Yield Criterion And Nonlinearly Hardening Rotating Shafts, Acta Mechanica 168, 129–144, 2004.

[9] Eraslan A.N., Mack W., A Computational Procedure For Estimating Residual Stresses And Secondary Plastic Flow Limits In Nonlinearly Strain Hardening Rotating Shafts, Forschung im Ingenieurwesen 69, 65–75, 2005.

[10] Akış T., Eraslan A.N., Yielding of Long Concentric Tubes under Radial Pressure Based on von Mises Criterion, Gazi Üni. Müh. Mim. Fak. Derg. Vol. 20, No. 3, 365–372, 2005.

[11] Eraslan A.N., Akış T., Deformation Analysis of Elastic-Plastic Two Layer Tubes Subject to Pressure: an Analytical Approach, Turkish J. Eng. Env. Sci. 28, 261–268, 2004.

[12] Eraslan A.N., Akış T., Yielding of Two-Layer Shrink-Fitted Composite Tubes Subject to Radial Pressure, Forsch Ingenieurwes 69, 187–196, 2005.

[13] Akış T., Eraslan A.N., The Stress Response and Onset of Yield Of Rotating FGM Hollow Shafts, Acta Mechanica 187, 169–187, 2006.

[14] Akış T., Eraslan A.N., Exact Solution of Rotating FGM Shaft Problem in The Elastoplastic State Of Stress, Arch Appl Mech 77, 745–765, 2007.

[15] Eraslan A.N., Akış T., On The Plane Strain and Plane Stress Solutions of Functionally Graded Rotating Solid Shaft and Solid Disk Problems, Acta Mechanica 181, 43–63, 2006.

[16] Argeşo, H., Eraslan A.N., A Computational Study on Functionally Graded Rotating Solid Shafts: Analysis of Preliminary Results, III European Conference on Computational Mechanics Solids, Structures and Coupled Problems in Engineering C.A. Mota Soares et al. (eds.) Lisbon, Portugal, 5–8, June 2006.